

Crystal Structure Engineering by Fine-Tuning the Surface Energy: The Case of CdE (E = S/Se) Nanocrystals

Angshuman Nag,^{ll,†} Abhijit Hazarika,[†] K. V. Shanavas,[‡] Surinder M. Sharma,[‡] I. Dasgupta,[§] and D. D. Sarma^{*,†}

[†]Solid State and Structural Chemistry Unit, Indian Institute of Science, Bangalore 560 012, India

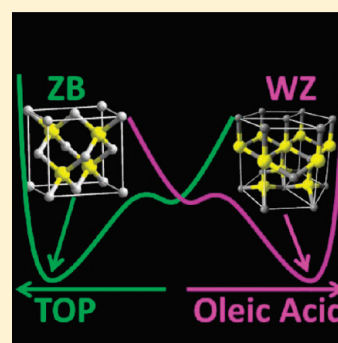
[‡]High Pressure and Synchrotron Radiation Physics Division, Bhabha Atomic Research Centre, Mumbai 400 085, India

[§]Department of Solid State Physics and Centre for Advanced Materials, Indian Association for the Cultivation of Science, Jadavpur, Kolkata 700 032, India

S Supporting Information

ABSTRACT: We prove that CdS nanocrystals can be thermodynamically stabilized in both wurtzite and zinc-blende crystallographic phases at will, just by the proper choice of the capping ligand. As a striking demonstration of this, the largest CdS nanocrystals (~15 nm diameter) ever formed with the zinc-blende structure have been synthesized at a high reaction temperature of 310 °C, in contrast to previous reports suggesting the formation of zinc-blende CdS only in the small size limit (<4.5 nm) or at a lower reaction temperature (≤ 240 °C). Theoretical analysis establishes that the binding energy of trioctylphosphine molecules on the (001) surface of zinc-blende CdS is significantly larger than that for any of the wurtzite planes. Consequently, trioctylphosphine as a capping agent stabilizes the zinc-blende phase via influencing the surface energy that plays an important role in the overall energetics of a nanocrystal. Besides achieving giant zinc-blende CdS nanocrystals, this new understanding allows us to prepare CdSe and CdSe/CdS core/shell nanocrystals in the zinc-blende structure.

SECTION: Nanoparticles and Nanostructures



Synthesis^{1–3} of high-quality semiconductor nanocrystals (NCs) of CdS and CdSe of varying size and shape have led to extensive studies^{4,5} of their electronic and optical properties, resulting in the use of these NCs in various novel applications.^{6,7} The crystal structure of NCs is also known to affect their properties substantially,^{8,9} including changes in the band gap¹⁰ and, consequently, in optical properties. Polyttypism, or the existence of two or more crystal structures in different domains of the same NC, has been used to prepare branched NCs, such as a tetrapod.¹¹ Effect of size, shape, and surface on the crystal structure of some semiconductor NCs was studied involving solid–solid phase transition by applying high pressure.^{12,13} Co NCs have been reported in a crystal phase that does not exist for the bulk counterpart.¹⁴ However, manipulation of the crystallographic phase of NCs has remained relatively less explored, mainly because of the inability to control the crystal structure during synthesis.

In the bulk form, wurtzite (WZ) is the thermodynamically stable phase for both CdS and CdSe, but the energy difference between the WZ and metastable zinc-blende (ZB) phases is only a few milli-electron volts per atom.^{11,15} Accordingly, syntheses of colloidal CdS and CdSe NCs generally lead to the stable WZ structure as in the bulk;^{1,2,16} however, formation of CdSe^{17–19} and CdS^{20–23} NCs in the less stable ZB structure have also been reported at times. Generally, a lower reaction temperature (<240 °C) has been considered^{17,21} to be the primary route to kinetically achieving the metastable ZB structure. In a contrasting explanation, Banerjee et al.²⁴ suggested a size-dependent phenomenon, with ZB being the stable form of CdS NCs for

sizes less than ~4.5 nm and the WZ structure being the ground state for NCs with sizes larger than ~4.5 nm. Although similar phase change was also observed by Al-Salim et al.²⁵ for CdSeS NCs, these results were interpreted differently; it was suggested that noncoordinating solvents are required to stabilize the ZB structure, whereas coordinating solvents favor WZ structure. Gautam et al.²⁶ were able to prepare ZB CdS NCs using solvothermal synthesis; in this case, the high pressure generated inside the autoclave was considered as a possible cause for stabilizing the ZB structure. In yet another attempt, ZB CdSe NCs had to be grown as an epitaxial layer on top of the structurally stable ZB form of ZnSe NC cores.²⁷ Clearly, various hypotheses to explain the formation of the “metastable” ZB phase put forward by different groups are divergent. In the absence of a clear understanding of the controlling parameters for the formation of ZB nanocrystalline CdS and CdSe, the synthesis of ZB heterostructured NCs involving CdSe and CdS, (e.g., CdSe/CdS core/shell NCs) are indeed rare in spite of the huge success in synthesizing their WZ counterparts and limited reports of binary CdSe and CdS NCs with the ZB structure.²⁸

In our efforts to understand parameters governing the crystal structure stability of NCs, we first establish that CdS NCs can be synthesized in different crystal structures with widely different sizes, under slightly varied reaction conditions. Unlike previous

Received: January 13, 2011

Accepted: February 21, 2011

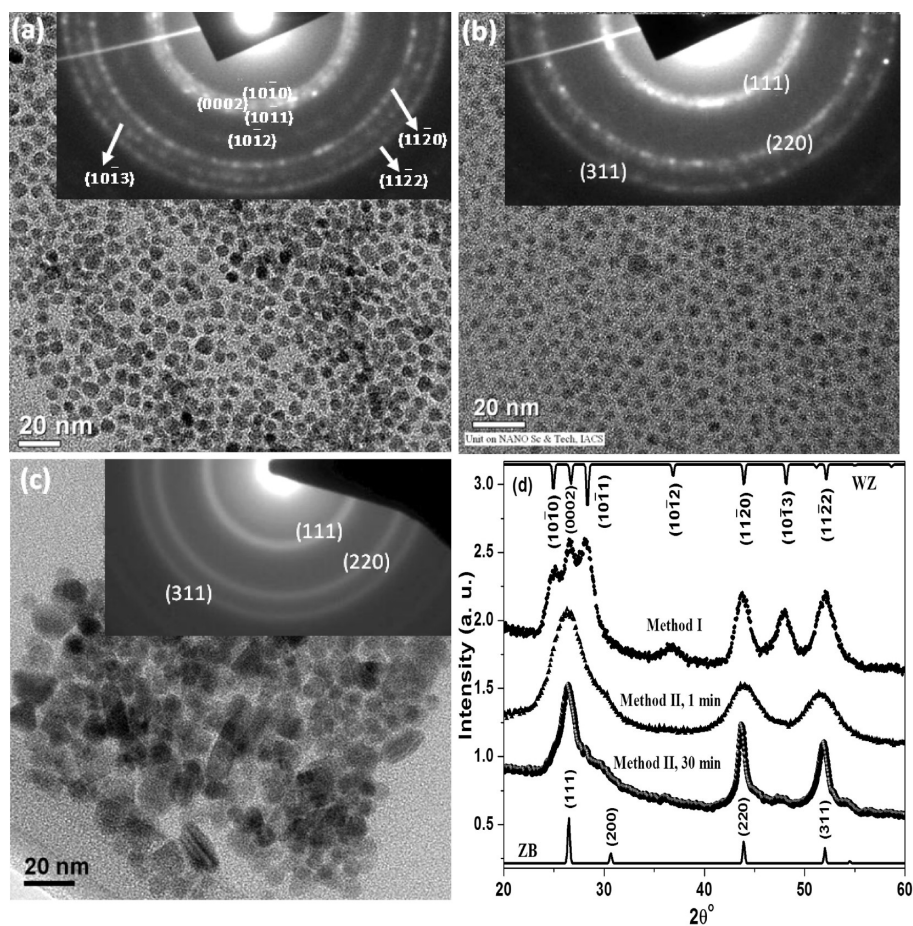


Figure 1. TEM images of CdS NCs prepared using (a) Method I (b) Method II for 1 min reaction time, and (c) Method II for 30 min reaction time. Insets of panels a, b, and c show SAED patterns of corresponding samples. (d) XRD patterns of CdS NCs synthesized using different reaction conditions; XRD patterns are shifted vertically for a clear presentation.

reports in the literature, here ZB NCs are formed at an unprecedented high reaction temperature of up to 310 °C and in a giant size limit up to ~ 15 nm. We show that primarily the presence or absence of trioctylphosphine (TOP) in the reaction medium controls the formation of either ZB or WZ CdS NCs, respectively. First principles electronic structure calculations reveal the binding mechanism of the organic capping agents on various terminations of ZB and WZ surfaces of a CdS crystal. The experimental and theoretical results show that binding energies of organic capping agents on the surface of the NCs are responsible for thermodynamically stabilizing the otherwise metastable ZB crystal structure in CdS NCs; in contrast, all other synthetic control parameters, such as the temperature, pressure, reaction time, and solvent, can at best influence the reaction path to kinetically achieve metastable states. The applicability of this microscopic understanding was illustrated by devising simple synthetic protocols that produce pure CdSe NCs, and CdSe/CdS core/shell NCs, in the relatively rare ZB crystal form.

To prepare NCs of CdS and CdSe in the two different crystal structures, we have employed two different methods of synthesis, which differ in the anionic reaction mixture: Method I involves S dissolved in 1-octadecene (ODE), while Method II involves S and/or Se dissolved separately in TOP as the reaction mixture. However, the initial Cd^{2+} -solution is common for both methods prepared by heating a mixture of CdO, oleic acid, and ODE. Details of the experimental conditions are described in the

Supporting Information (SI). A typical reaction of CdS NCs using Method I is similar to that reported in ref 16: 1 mL of oleylamine was injected to the above Cd^{2+} -solution, followed by the addition of S solution (S in ODE) at 310 °C, and the reaction was continued for 20 min. For the second method of synthesis of CdS NCs, TOP-S was added to Cd^{2+} solution, similar to ref 29. It is to be noted that the primary solvent to carry out the synthesis is ODE in both methods, with a small amount of TOP only in the case of Method II. In addition, we have also prepared CdSe NCs and CdSe/CdS core/shell NCs using Method II. Core/shell NCs were prepared by modifying the successive ion layer adsorption and reaction (SILAR) method reported in ref 30.

The transmission electron microscopy (TEM) image in Figure 1a shows that the NC synthesized using Method I has an average diameter of 6.8 nm, with a size distribution of 8%. Figure 1b,c shows that the NCs synthesized using Method II with reaction times of 1 and 30 min exhibit average diameters of 4.5 (9% size distribution) and ~ 15 nm, respectively; in other words, one smaller and one larger than particles obtained by Method I. By tuning the reaction time between 1 and 30 min, it is possible to form intermediate sizes. This increase in NC size with an increase in the reaction time for Method II is also reflected by a decrease in the optical gap from 2.66 eV (467 nm) at 1 min to 2.48 eV (500 nm) at 30 min, as shown by the absorption and emission spectra in Figure S1 of the SI. While Figure 1a,b shows nearly spherical NCs, Figure 1c exhibits some NCs with a

nonspherical (prolate) shape. Thus, during the ripening process in Method II (for 30 min), NCs not only grow larger in size, but also different shapes evolve; occasionally we also found very large particles with sizes up to ~ 25 nm.

Insets to Figure 1a–c show the corresponding selected area electron diffraction (SAED) patterns. CdS NCs synthesized using Method I (inset to Figure 1a) exhibit four distinctly visible rings for $(10\bar{1}2)$, $(11\bar{2}0)$, $(10\bar{1}3)$, and $(11\bar{2}2)$ reflections along with a broad ring due to superimposition of $(10\bar{1}0)$, (0002) , and $(10\bar{1}1)$ reflections of WZ CdS NCs. However, both samples of CdS NCs synthesized using Method II (insets to Figure 1b,c) exhibit a clear three-ring pattern, showing (111) , (220) , and (311) planes of the ZB CdS NCs.

Figure 1d presents powder X-ray diffraction (XRD) patterns of CdS NCs synthesized using Methods I and II. A comparison of the XRD patterns of CdS NCs with WZ and ZB patterns of bulk CdS (shown by solid lines in Figure 1d) shows that NCs synthesized by Method I exhibit WZ structure, while those synthesized by Method II exhibit ZB structure, in agreement with the SAED results presented in Figure 1a–c. Three distinct features at $2\theta = 26.5^\circ$, 43.9° , and 52° for CdS NCs prepared by Method II are the characteristics of (111) , (220) , and (311) reflections of the ZB phase, respectively. Although the $(10\bar{1}0)$, (0002) , and $(10\bar{1}1)$ reflections of WZ structure might lead to a single broad peak for small NCs, the absence of $(10\bar{1}2)$ and $(10\bar{1}3)$ peaks at $2\theta = 36.8^\circ$ and 48.1° , respectively, for samples prepared using Method II is clear evidence for the formation of ZB structure. In particular, CdS NCs of size ~ 15 nm prepared by Method II that exhibit narrow diffraction peaks show the clear evidence of ZB structure. It is to be noted that, CdS NCs prepared by Method II at different temperatures in the range of 200 – 310 °C also exhibit ZB crystal structure. On the other hand, the sample prepared by Method I shows diffraction peaks at $2\theta = 25.0^\circ$, 26.6° , 28.2° , 36.8° , 43.9° , 48.1° , and 52.1° , clearly establishing the WZ structure. We note that the absence or presence of oleylamine in both Methods I and II do not influence the obtained crystal structure (Figure 1d and Figure S2 in the SI); however, addition of oleylamine in Method I provides a better monodispersity in the size and shape of the synthesized NCs.

Figure 2a shows a representative high-resolution TEM (HRTEM) image of a single NC prepared by Method I, reflecting its atomic arrangement. The (0002) plane of the WZ phase with an interplanar distance of 3.33 Å is shown in the image. More importantly, the characteristic ABABAB stacking sequence of the hexagonal WZ structure along the $[0001]$ (equivalently $[0002]$) direction, shown by the arrow, is clearly observed (Figure 2a). The $(11\bar{2}0)$ planes with an interplanar distance of 2.07 Å is also shown in Figure 2a. Fast Fourier transform (FFT) of the HRTEM image of Figure 2a is shown in Figure 2b. Clearly, two hexagons can be constructed from the FFT pattern, with equidistant dots from the zone axis and an angle of 60° between any two adjacent dots through the zone axis for a given hexagon. All the spots in the FFT pattern have been assigned to different WZ planes with $[0001]$ zone axis. Thus, Figure 2a,b unambiguously establishes the formation of defect-free, single crystalline CdS NCs with WZ phase. Figure 2c,d respectively shows the HRTEM image and the corresponding FFT pattern of a CdS NC synthesized by Method II for a reaction time of 1 min. The observed interplanar distances (Figure 2c) of 3.35 , 2.93 , and 2.03 Å are attributed to (111) , (200) , and (220) reflections, respectively, of CdS NCs in the ZB phase. It is to be noted that the

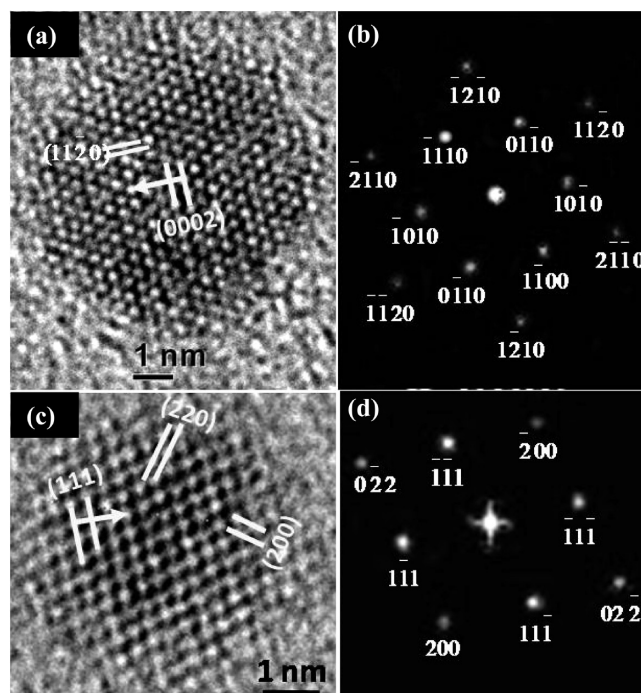


Figure 2. (a) HRTEM image and (b) FFT pattern of a CdS NC prepared with Method I. (c,d) HRTEM image and FFT pattern of a CdS NC prepared by Method II for 1 min reaction time.

observation of an interplanar distance of 2.93 Å is unique for ZB CdS, since there is no corresponding WZ plane with a similar interplanar distance. The ABCABC stacking sequence along the $[111]$ direction of a ZB structure is shown by the arrow in Figure 2c. All the spots in the corresponding FFT pattern, shown in Figure 2d, have been assigned to different planes of a ZB structure, with a zone axis of $[001]$. The ratio of interplanar distances, $d_{220}:d_{200}:d_{111}$, obtained from the FFT pattern (Figure 2d) is $1:1.37:1.62$, and agrees well (within 3%) with the expected values ($1:1.41:1.63$). Also, the angles between the $(\bar{1}\bar{1}1)$ plane and the $(\bar{2}00)$, $(1\bar{1}1)$, and $(0\bar{2}2)$ planes, obtained from Figure 2d, are 55° , 71° , and 36° again match the expected values of a ZB structure. Therefore, it is evident that CdS NCs prepared by Method II exhibit defect-free single crystalline ZB structure, even for a reaction time as small as 1 min.

Above results suggest that WZ and ZB are the thermodynamic ground states of CdS NCs prepared under reaction conditions of Methods I and II, respectively. Further, dispersions of both these samples were annealed at 310 °C for a long time in order to achieve the thermodynamic ground state; both crystallographic forms retained their original structures in spite of such heating. In contrast to previously reported results, we achieve these two crystallographic forms independent of any possible influences from solvent effect,²⁵ temperature effect,^{17–22} pressure effect,²⁶ and NC size effect,²⁴ as we keep these parameters the same in both synthetic methods. The only difference in the two synthetic methods is the additional presence of TOP in Method II. Since TOP is an effective capping agent for cadmium chalcogenide nanoparticles, it is quite likely that TOP will take part in passivating the NCs in Method II. Thus, it appears that TOP as a capping agent plays an important role in stabilizing the ZB structure, with the expected WZ structure indeed being the ground state in the absence of any TOP.

In view of the above, we varied the amount of TOP in the reaction mixture, and found that the structure remains WZ for up to 0.75 mL of TOP (Figure S3 in the SI), and the ZB structure is formed for ≥ 1 mL of TOP, supporting the view that TOP is crucial in stabilizing the ZB structure. It is curious to note in this context that TOP-E (E = S, Se) has been commonly used in the synthesis of WZ CdE NCs for many years in an apparent contradiction to our results. However, in most of these cases, TOP-E was used along with other stronger ligands such as tri-*n*-octylphosphonic oxide (TOPO) and/or alkylphosphonic acid.^{1,31} Our reading of the literature, however, shows that in the absence of TOPO and alkylphosphonic acid, TOPE almost always resulted into the ZB structure over widely different reaction conditions, while the explanation offered in these publications for forming this usually less stable phase was variously attributed to a low reaction temperature (240 °C),¹⁹ noncoordinating solvent,²⁵ and the microwave-based synthesis condition.³² Our ability to tune the crystal structure just by the presence or the absence of TOP in an otherwise fixed reaction condition, together with the past literature, therefore, strongly suggests that TOP allows one to stabilize the usually metastable ZB structure of CdS NCs.

In order to understand the origin of this experimental observation, we note that the stability of the crystal structure of NCs is contributed significantly by the surface energy, whose importance gradually decreases with an increasing size of the NC. Datta et al.³³ have indeed shown theoretically that the surface contribution can lead to a transformation between ZB and WZ structure for small (<2 nm) uncapped CdS NCs. It is important to note here that it is difficult to influence the Cd–S bonding within the core region of an NC, thereby affording no control to tune the volume energy contribution to the total energy of a NC. By contrast, the surface energy contribution is amenable to fine-tuning by the control of the NC–capping agent interaction.

On the basis of the above discussion, one plausible mechanism to stabilize the ZB structure for CdS NCs with TOP-S as the S precursor is based on the possibility of a larger binding energy of the TOP molecule on ZB surfaces in comparison to that on WZ surfaces of CdS NCs. In order to critically examine the above possibility, binding energies of TOP and oleic acid for various terminations of ZB and WZ surfaces of CdS are calculated using density functional theory. The electronic wave functions are expanded on a plane wave basis set and ionic core states are approximated by using the projected augmented wave (PAW) method as implemented in the Vienna ab initio simulation package (VASP).^{34,35} We have applied the generalized gradient approximation (GGA) to the exchange correlation functional with Perdew–Burke–Ernzerhof (PBE) parametrization.^{36,37} Details of the computational methodology is given in the SI. We considered (110), (001), (111A), and (111B) surfaces for ZB and (11 $\bar{2}$ 0), (10 $\bar{1}$ 0), (0001A), and (0001B) surfaces for WZ structures,²⁷ with “A” and “B” representing to S-rich and Cd-rich terminations of the surfaces, respectively. To make the problem computationally viable, we approximate the three long hydrocarbon chains in TOP and one in cis-OA molecules after the functional group by ethyl groups (CH₃–CH₂–). Since we do not change the functional group that attaches to the surface, this approximation is not expected to affect our computational results.³⁸

In Figure 3a,b we show binding energies of the TOP molecule for various terminations of ZB and WZ surfaces, respectively. These results clearly reveal that TOP prefers ZB crystal structure, affording an overall higher binding energy for surface capping.

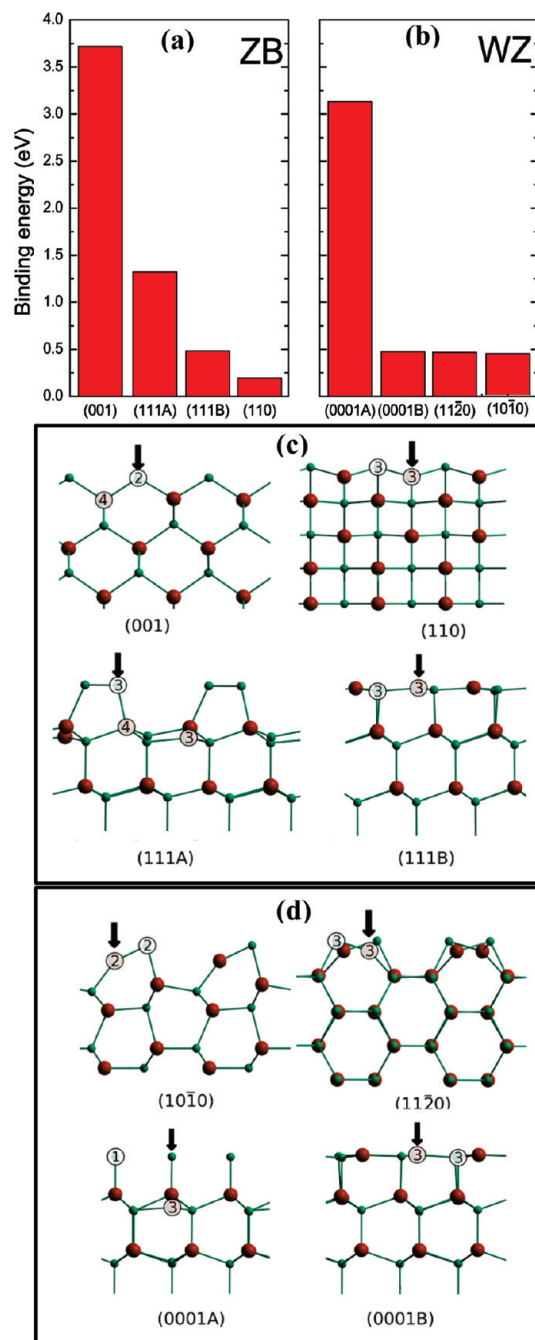


Figure 3. Binding energies of TOP on various surfaces of (a) ZB and (b) WZ structures. “A” and “B” represent S-rich and Cd-rich terminations of surfaces, respectively. Reconstructed surfaces of (c) ZB and (d) WZ viewed along the *a* direction. Large red spheres represent Cd atoms, while smaller green spheres are S atoms. Arrows show the site at which TOP adsorbs. Coordination numbers of the surface atoms are marked in the figure.

Thus, TOP binding on the surface of CdS NC prefers the NC to be in the ZB form, thereby providing us with the microscopic origin of our experimental observation in terms of the energetic. While the noncoordinating ODE does not participate in the reaction as a capping agent, however, the oleic acid present in the Cd²⁺ precursor solution in both the methods of synthesis can act as a capping agent. Our calculations (Figure S4 in the SI) show that, unlike TOP, oleic acid does not favor the ZB structure

supporting the synthesis of WZ CdS NCs using Method I. It is evident from the results in Figure 3a,b that TOP interacts with surface S atoms of CdS (A-type termination) more strongly than with the surface Cd atoms (B-type termination) independent of the crystal structure. In the following, we analyze this observation in some detail.

Figure 3c,d shows reconstructed ZB and WZ surfaces as well as the lowest energy binding sites for the TOP molecule. These surfaces relax further upon molecular binding; these additional distortions are not relevant for the present discussion and, consequently, are not shown here. In bulk ZB and WZ structure, Cd and S atoms form a tetrahedral structure where each Cd (S) has four S (Cd) atoms as neighbors. On the surface, due to the broken periodicity, the coordination number of Cd and S are reduced, resulting in dangling bonds given by $(4 - z_i)$ where z_i is the local coordination of either Cd or S as shown in Figure 3c,d. As a result when a TOP molecule approaches the surface, the dominant bonding interaction is expected between P of the TOP molecule and unsaturated S sites on the surface. As anticipated, it is found that TOP binds most strongly with the bicoordinated S in the ZB 001 surface. Among the WZ surfaces, TOP binds with the S in the 0001A surface where the coordination of the S atom is 1; however, this binding is weaker in comparison to ZB (001) (see Figure 3a,b). A plot of the charge density shown in Figure S5 in the SI reveals that, for a TOP molecule on a WZ (0001A) surface, there is a single Cd–S bond resulting in three S dangling bonds. A single TOP molecule cannot saturate all the S dangling bonds, and the P–S–Cd bond angle approaches the linear limit (175°), which is much larger than a typical Cd–S–Cd bond angle (109°) in the bulk CdS. This results in the weakening of Cd–S bond (shown by the dotted line). On the contrary, for a TOP molecule on the 001 ZB surface, the binding of the TOP molecule strengthens the bonding as it saturates all the S dangling bonds, with the P–S–Cd bond angle (124°) forming close to the bulk Cd–S–Cd bond angle. Consequently, ZB CdS NCs form as the stable form when TOP-S is used as the S precursor in Method II. In a larger context, our theoretical results suggest that the surface topology, the specific nature of the capping molecule, the coordination of surface atoms where the capping molecule is likely to attach itself, and the conformation of the capping molecule play key roles in determining the energetics and therefore in the surface molecular binding, eventually influencing the stability of the NCs including its structure type in any given synthetic procedure. Consequently, ZB CdS NCs were prepared when TOP-S is used as the S precursor in Method II.

The surface energy contribution to the total energy must decrease with an increase in the NC size, as already pointed out before. Thus, one would not expect the ZB structure to continue as the thermodynamically stable phase beyond a critical size. In order to probe this aspect, the intrinsic distribution of NC size in a given reaction within Method II was used to find stray cases of particle sizes considerably larger than the average size of 15 nm. Figure 4a,b exhibits HRTEM images of two typical particles, one with ~ 15 nm diameter and the other ~ 25 nm, respectively. Insets to Figure 4a showing the magnified view of a small part of the image in the mainframe for the 15 nm NC highlight the ABCABC stacking sequence of ZB CdS. However, the 25 nm NC in Figure 4b clearly exhibits ABABAB stacking sequence, as shown in the inset of the Figure 4b. FFT patterns (not shown here) of the HRTEM images of these NCs in Figure 4a,b establish the ZB and WZ structures for the 15 and 25 nm CdS

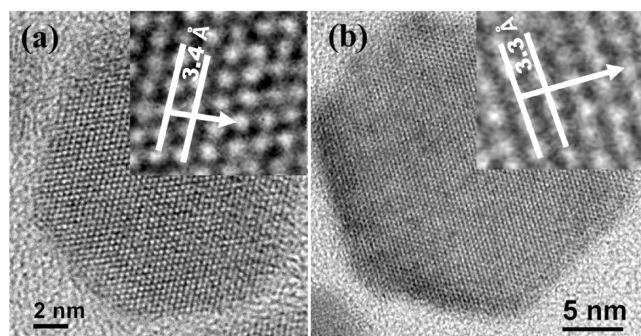


Figure 4. HRTEM images of two different NCs (a and b) taken from the product of the same reaction, Method II with 30 min reaction time. Insets to panels a and b show the magnified view of a small region of the corresponding mainframe, showing ABCABC and ABABAB stacking sequences along the [111] and [0001] directions of ZB and WZ structure, respectively.

NCs, respectively. This observation suggests a size-dependent phase change in the CdS crystal with a critical size between 15 and 25 nm in the presence of TOP, while thiophenol-capped CdS nanoparticles are estimated to have a critical size of about 4.5 nm.²²

On the basis of these results, one can conclude that a suitable choice of the capping material can be very effectively used to engineer a specific crystal structure and extend its stability range over a large regime of NC sizes. It is also obvious that only the choice of the capping agent in the synthetic reaction has the ability to tilt the energy balance in favor of a usually metastable state for a NC, thereby converting that into the thermodynamically stable state, whereas all other control parameters such as the reaction time, temperature, pressure, and noncoordinating solvent can only favor the metastable state by kinetically altering the reaction path.

Generalizing this approach of crystal phase engineering by using TOP's enhanced binding on ZB surfaces compared to WZ surfaces, we have also stabilized the ZB structure for CdSe and CdSe/CdS NCs by using TOP-Se/TOP-S as the source of Se/S in the reaction mixture. While there are only few reports^{16–18} of CdSe NCs in the ZB form, this strategy has allowed us to stabilize as large as 6.5 nm diameter (TEM image in Figure S6 of the SI) CdSe NCs in the cubic ZB structure, as shown by the XRD pattern in Figure S7 of the SI. The SAED pattern (inset to Figure S6 in the SI) exhibits the characteristic three ring pattern for ZB NCs. We are also able to tune the size of these CdSe NCs synthesized in the ZB structure by tuning the reaction temperature in the range of 200–300 °C, thereby varying the average diameter over the range of 3.5–6.5 nm. This property is evidently a more direct method of obtaining the ZB form of CdSe than stabilizing²⁷ this phase as thin films by growing on top of a ZnSe ZB NC. The fact that the preparation of ZB heterostructured NCs containing CdSe and CdS has proven to be difficult²⁸ motivated us to prepare CdSe/CdS core/shell NCs exhibiting ZB structure. Clearly, CdSe/CdS core/shell NCs (average diameter 8.8 nm) with 5.6 nm CdSe core and five monolayers of CdS shell prepared by the SILAR method within our approach exhibit a ZB structure, as shown by the XRD pattern in Figure S7 in the SI. The lattice parameters of the CdSe/CdS core/shell NCs appear in between those of the bulk CdSe and CdS, and can be tuned by controlling the relative contributions of CdS and CdSe in the NC, as has been reported

previously for core/shell structures in the WZ form.³⁰ It is to be noted that previous attempts²⁸ to prepare ZB CdSe/CdS core/shell NCs by using a ZB CdSe core were not successful using the SILAR method, while this method is known to be one of the most successful methods to prepare core/shell NCs with the WZ structure.

In conclusion, we have shown that an appropriate choice of the ligand alone (TOP, in this case) is sufficient to thermodynamically stabilize the otherwise uncommon and metastable ZB form of CdS and CdSe NCs as well as their core-shell structures in highly single crystalline forms without the presence of any defect or polytypism. Combination of experiment and theory establishes that the surface binding energy of the ligand molecule on various surfaces of these NCs plays the most crucial role in stabilizing the unusual ZB structure. Using this NC surface-capping molecule interaction as a tool, we have been able to prepare the largest CdS NCs (15 nm) with the ZB structure. However, with a further increase in the particle size up to 25 nm, CdS NCs are found to convert to the WZ phase, because the contribution of the surface energy to the total energy of the NC decreases with increasing NC size.

ASSOCIATED CONTENT

S Supporting Information. UV-visible absorption, Photoluminescence spectra and XRD pattern for CdS, CdSe, and CdSe/CdS core/shell NCs. Binding energies of oleic acid on WZ CdS and Charge density plots for adsorption of TOP. TEM image, along with SAED pattern CdSe NCs. This information is available free of charge via the Internet at <http://pubs.acs.org/>.

AUTHOR INFORMATION

Corresponding Author

*E-mail: sarma@sscu.iisc.ernet.in. Also with Jawaharlal Nehru Centre for Advanced Scientific Research, Bangalore 560054, India.

Present Addresses

¹¹Department of Chemistry, University of Chicago, Chicago, Illinois 60637, United States.

ACKNOWLEDGMENT

Authors acknowledge Department of Science and Technology, Government of India, for funding the project. D.D.S. acknowledges a J. C. Bose National Fellowship.

REFERENCES

- (1) Murray, C. B.; Norris, D. J.; Bawendi, M. G. Synthesis and Characterization of Nearly Monodisperse CdE (E = Sulfur, Selenium, Tellurium) Semiconductor Nanocrystallites. *J. Am. Chem. Soc.* **1993**, *115*, 8706–8715.
- (2) Qu, L.; Peng, Z. A.; Peng, X. Alternative Routes toward High Quality CdSe Nanocrystals. *Nano Lett.* **2001**, *1*, 333–337.
- (3) Karan, N. S.; Sarma, D. D.; Kadam, R. M.; Pradhan, N. Doping Transition Metal (Mn or Cu) Ions in Semiconductor Nanocrystals. *J. Phys. Chem. Lett.* **2010**, *1*, 2863–2866.
- (4) Talapain, D. V.; Neloson, J. H.; Shevchenko, E. V.; Aloni, S.; Sadtler, B.; Alivisatos, A. P. Seeded Growth of Highly Luminescent CdSe/CdS Nanoheterostructures with Rod and Tetrapod Morphologies. *Nano Lett.* **2007**, *7*, 2951–2959.
- (5) Sarma, D. D.; Nag, A.; Santra, P. K.; Kumar, A.; Sapra, S.; Mahadevan, P. Origin of the Enhanced Photoluminescence from

Semiconductor CdSeS Nanocrystals. *J. Phys. Chem. Lett.* **2010**, *1*, 2149–2153.

(6) Farrow, B.; Kamat, P. V. CdSe Quantum Dot Sensitized Solar Cells. Shuttling Electrons Through Stacked Carbon Nanocups. *J. Am. Chem. Soc.* **2009**, *131*, 11124–11131.

(7) Nag, A.; Kumar, A.; Kiran, P. P.; Chakraborty, S.; Kumar, G. R.; Sarma, D. D. Optically Bifunctional Heterostructured Nanocrystals. *J. Phys. Chem. C* **2008**, *112*, 8229–8233.

(8) Viswanatha, R.; Sapra, S.; Saha-Dasgupta, T.; Sarma, D. D. Electronic Structure of and Quantum Size Effect in III-V and II-VI Semiconducting Nanocrystals Using a Realistic Tight Binding Approach. *Phys. Rev. B* **2005**, *72*, 045333.

(9) Yang, Y. A.; Wu, H.; Williams, K. R.; Cao, Y. C. Synthesis of CdSe and CdTe Nanocrystals without Precursor Injection. *Angew. Chem., Int. Ed.* **2005**, *44*, 6712–6715.

(10) Viswanatha, R.; Sarma, D. D. Effect of Structural Modification on the Quantum-Size Effect in II–VI Semiconducting Nanocrystals. *Chem. Asian J.* **2009**, *4*, 904–909.

(11) Manna, L.; Milliron, D. J.; Meisel, A.; Scher, E. C.; Alivisatos, A. P. Controlled Growth of Tetrapod-Branched Inorganic Nanocrystals. *Nat. Mater.* **2003**, *2*, 382–385.

(12) Tolbert, S. H.; Herhold, A. B.; Brus, L. E.; Alivisatos, A. P. Pressure-Induced Structural Transformations in Si Nanocrystals: Surface and Shape Effects. *Phys. Rev. Lett.* **1996**, *76*, 4384–4387.

(13) Chen, C. C.; Herhold, A. B.; Johnson, C. S.; Alivisatos, A. P. Size Dependence of Structural Metastability in Semiconductor Nanocrystals. *Science* **1997**, *276*, 398–401.

(14) Sun, S.; Murray, C. B. Synthesis of Monodisperse Cobalt Nanocrystals and their Assembly into Magnetic Superlattices. *J. Appl. Phys.* **1999**, *85*, 4325–4330.

(15) Yeh, Y.; Lu, Z. W.; Froyen, S.; Zunger, A. Zinc-Blende–Wurtzite Polytypism in Semiconductors. *Phys. Rev. B* **1992**, *46*, 10086–10097.

(16) Nag, A.; Chakraborty, S.; Sarma, D. D. To Dope Mn²⁺ in a Semiconducting Nanocrystal. *J. Am. Chem. Soc.* **2008**, *130*, 10605–10611.

(17) Mohamed, M. B.; Tonti, D.; Al-Salman, A.; Chemseddine, A.; Chergui, M. Synthesis of High Quality Zinc Blende CdSe Nanocrystals. *J. Phys. Chem. B* **2005**, *109*, 10533–10537.

(18) Deng, Z.; Cao, L.; Tang, F.; Zou, B. A New Route to Zinc-Blende CdSe Nanocrystals: Mechanism and Synthesis. *J. Phys. Chem. B* **2005**, *109*, 16671–16675.

(19) Han, L.; Qin, D.; Jiang, X.; Liu, Y.; Wang, L.; Chen, J.; Cao, Y. Synthesis of High Quality Zinc-Blende CdSe Nanocrystals and Their Application in Hybrid solar cells. *Nanotechnology* **2006**, *17*, 4736–4742.

(20) Vossmeier, T.; Katsikas, L.; Gienig, M.; Popovic, I. G.; Diesner, K.; Chemseddine, A.; Eychmüller, A.; Weller, H. CdS Nanoclusters: Synthesis, Characterization, Size Dependent Oscillator Strength, Temperature Shift of the Excitonic Transition Energy, and Reversible Absorbance Shift. *J. Phys. Chem.* **1994**, *98*, 7665–7673.

(21) Cao, Y. C.; Wang, J. One-Pot Synthesis of High-Quality Zinc-Blende CdS Nanocrystals. *J. Am. Chem. Soc.* **2004**, *126*, 14336–14337.

(22) Pan, D.; Jiang, S.; An, L.; Jiang, B. Controllable Synthesis of Highly Luminescent and Monodisperse CdS Nanocrystals by a Two-Phase Approach under Mild Conditions. *Adv. Mater.* **2004**, *16*, 982–985.

(23) Srivastava, B. B.; Jana, S.; Sarma, D. D.; Pradhan, N. Surface Ligand Population Controlled Oriented Attachment: A Case of CdS Nanowires. *J. Phys. Chem. Lett.* **2010**, *1*, 1932–1935.

(24) Banerjee, R.; Jayakrishnan, R.; Ayyub, P. Effect of the Size-Induced Structural Transformation on the Band Gap in CdS Nanoparticles. *J. Phys.: Condens. Matter* **2000**, *12*, 10647–10654.

(25) Al-Salim, N.; Young, A. G.; Tilley, R. D.; McQuillan, A. J.; Xia, J. Synthesis of CdSeS Nanocrystals in Coordinating and Noncoordinating Solvents: Solvent's Role in Evolution of the Optical and Structural Properties. *Chem. Mater.* **2007**, *19*, 5185–5193.

(26) Gautam, U. K.; Seshadri, R.; Rao, C. N. R. A Solvothermal Route to CdS Anocrystals. *Chem. Phys. Lett.* **2003**, *375*, 560–564.

- (27) Erwin, S. C.; Zu, L.; Haftel, M. I.; Efros, A. L.; Kennedy, T. A.; Norris, D. J. Doping Semiconductor Nanocrystals. *Nature* **2005**, *436*, 91–94.
- (28) Mahler, B.; Lequeux, N.; Dubertret, B. Ligand-Controlled Polytypism of Thick-Shell CdSe/CdS Nanocrystals. *J. Am. Chem. Soc.* **2010**, *132*, 953–959.
- (29) Yu, W. W.; Peng, X. Formation of High-Quality CdS and Other II-VI Semiconductor Nanocrystals in Noncoordinating Solvents: Tunable Reactivity of Monomers. *Angew. Chem., Int. Ed* **2002**, *41*, 2368–2371.
- (30) Li, J. J.; Wang, Y. A.; Guo, W. Z.; Keay, J. C.; Mishima, T. D.; Johnson, M. B.; Peng, X. Large-Scale Synthesis of Nearly Monodisperse CdSe/CdS Core/Shell Nanocrystals Using Air-Stable Reagents via Successive Ion Layer Adsorption and Reaction. *J. Am. Chem. Soc.* **2003**, *125*, 12567–12575.
- (31) Peng, X.; Manna, L.; Yang, W.; Wickham, J.; Scher, E.; Kadavanich, A.; Alivisatos, A. P. Shape Control of CdSe Nanocrystals. *Nature* **2000**, *404*, 59–61.
- (32) Washington, A. L., II; Strouse, G. F. Microwave Synthetic Route for Highly Emissive TOP/TOP-S Passivated CdS Quantum Dots. *Chem. Mater.* **2009**, *21*, 3586–3692.
- (33) Datta, S.; Kabir, M.; Saha-Dasgupta, T.; Sarma, D. D. First-Principles Study of Structural Stability and Electronic Structure of CdS Nanoclusters. *J. Phys. Chem. C* **2008**, *112*, 8206–8214.
- (34) Kresse, G.; Hafner, J. *Ab initio* Molecular Dynamics for Liquid Metals. *Phys. Rev. B* **1993**, *47*, 558–561.
- (35) Kresse, G.; Furthmüller, J. Efficient Iterative Schemes for *Ab Initio* Total-Energy Calculations Using a Plane-Wave Basis Set. *Phys. Rev. B* **1996**, *54*, 11169–11186.
- (36) Perdew, J. P.; Burke, K.; Wang, Y. Generalized Gradient Approximation for the Exchange-Correlation Hole of a Many-Electron System. *Phys. Rev. B* **1996**, *54*, 16533–16539.
- (37) Perdew, J. P.; Burke, K.; Ernzerhof, M. Generalized Gradient Approximation Made Simple. *Phys. Rev. Lett.* **1996**, *77*, 3865–3868.
- (38) Puzder, A.; Williamson, A. J.; Zaitseva, N.; Galli, G.; Manna, L.; Alivisatos, A. P. The Effect of Organic Ligand Binding on the Growth of CdSe Nanoparticles Probed by *Ab Initio* Calculations. *Nano Lett.* **2004**, *4*, 2361–2365.